JAERI-Research
2004-010

GLOBAL CHARACTERISTICS OF ZONAL FLOWS GENERATED BY ION TEMPERATURE GRADIENT DRIVEN TURBULENCE IN TOKAMAK PLASMAS

August 2004

Naoaki MIYATO, Yasuaki KISHIMOTO and Jiquan LI

日本原子力研究所
Japan Atomic Energy Research Institute

本レポートは，日本原子力研究所が不定期に公刊している研究報告書です。
入手の問合わせは，日本原子力研究所研究情報部研究情報課（〒319－1195 茨城県那珂郡東海村）あて，お申し越しください。なお，このほかに財団法人原子力弘済会資料センター（〒319－1195 茨城県那珂郡東海村日本原子力研究所内）で複写による実費頒布をおこなっております。

This report is issued irregularly.
Inquiries about availability of the reports should be addressed to Research Information Division, Department of Intellectual Resources, Japan Atomic Energy Research Institute, Tokai-mura, Naka-gun, Ibaraki-ken 〒319－1195, Japan.

編集兼発行　日本原子力研究所

Global Characteristics of Zonal Flows Generated by Ion Temperature Gradient Driven Turbulence in Tokamak Plasmas

Naoaki MIYATO[※1], Yasuaki KISHIMOTO[※2] and Jiquan LI[※3]

Department of Fusion Plasma Research
Naka Fusion Research Establishment
Japan Atomic Energy Research Institute
Naka-machi, Naka-gun, Ibaraki-ken

(Received June 18, 2004)

Global structure of zonal flows driven by ion temperature gradient driven turbulence in tokamak plasmas is investigated using a global electromagnetic Landau fluid code. Characteristics of the coupled system of the zonal flows and the turbulence change with the safety factor q. In a low q region stationary zonal flows are excited and suppress the turbulence effectively. Coupling between zonal flows and poloidally asymmetric pressure perturbations via a geodesic curvature makes the zonal flows oscillatory in a high q region. Also we identify energy transfer from the zonal flows to the turbulence via the poloidally asymmetric pressure perturbations in the high q region. Therefore in the high q region the zonal flows cannot quench the turbulet transport completely.

Keywords: Zonal Flow, ITG Turbulence, GAM, Tokamak

[※1] Post-Doctoral Fellow
[※2] Invited Researcher
[※3] JAERI Research Fellow

トカマクプラズマ中のイオン温度勾配駆動乱流により作られる帯状流のグローバル特性

日本原子力研究所那珂研究所炉心プラズマ研究部
宮戸　直亮[※1]・岸本　泰明[※2]・李　継全[※3]

(2004年6月18日 受理)

トカマクプラズマ中のイオン温度勾配 (ITG) 駆動乱流によって作られる帯状流のグローバルな構造をグローバル電磁ランダウ流体コードによって調べた。この帯状流－ITG乱流結合系の性質は安全係数qにより変化する。qが小さな領域では、静的な帯状流が励起され、乱流を効果的に抑制する。一方、qが大きな領域では、ポロイダル非対称な圧力揺動との結合により帯状流は振動する。また、帯状流のエネルギーがポロイダル非対称な圧力揺動を通して乱流へ輸送されていることを同定した。これにより、qが大きな領域では帯状流が乱流輸送を完全に抑えることはできないことがわかった。

那珂研究所：〒311-0193　茨城県那珂郡那珂町向山801-1
※1 博士研究員
※2 客員研究員
※3 原研リサーチフェロー

Contents

目　次

1 Introduction

It is believed that drift wave turbulence such as ion temperature gradient (ITG) driven turbulence and the zonal flow [1] nonlinearly generated from it via Reynolds stress play an important role for anomalous transport in tokamak plasmas. The ITG turbulence is considered as the main candidate inducing anomalous ion heat transport in a core plasma. Zonal flows are poloidally and toroidally symmetric (m, n)=(0,0) flows, where m and n are poloidal and toroidal mode numbers, respectively. Global gyrokinetic simulations of ITG turbulence have demonstrated that turbulent ion transport in the interior region can be regulated by the zonal flows[2]. Originally considered zonal flows are low frequency and almost stationary compared to the timescale of turbulence. The stationary zonal flows can keep decorrelating turbulent vortices in long time and then turbulent transport is effectively suppressed. Therefore, intensive theoretical studies for zonal flow generation have been done in various drift waves [3, 4, 6, 7, 5, 8, 9]. Analytical theories for coupled system of the drift wave turbulence and the stationary zonal flows have also been developed[3, 4]. Zonal flows, however, may oscillate in time by coupling with poloidally asymmetric (m, n)=(1,0) pressure perturbations in toroidal system such as tokamak. The coupling is due to a geodesic curvature and the oscillation is called the geodesic acoustic mode (GAM)[10]. Local fluid simulations in a high q region near edge have shown that the zonal flows make a coherent oscillation at the GAM frequency[11, 13, 12]. Recently the GAMs are detected experimentally using heavy ion beam probe on Texas EXperimental Tokamak (TEXT)[14] and beam emission spectroscopy on Doublet III D (DIII-D)[15]. It is important whether zonal flows oscillate or not because the oscillatory zonal flows are less effective in suppressing the turbulence than the slowly time varying ones[16].

Moreover the coupling between the zonal flows and the (1,0) pressure perturbations opens another energy path between the zonal flows and the turbulence in addition to the Reynolds stress. The role of the path to the zonal flows was first discussed in three dimensional electrostatic Braginskii turbulence simulations in the core/edge transition regime[11]. The results of the simulations showed that zonal flows can be driven through the path from the turbulence. The path was also reported as a loss channel of the zonal flow energy in drift-Alfvén turbulence simulations[13, 12]. In this case it is difficult that the zonal flows become significant compared to the turbulence and quench the turbulent transport.

It is necessary for understanding the anomalous transport in the core to investigate the zonal flow behavior including nonlinear dynamics between the zonal flows and the turbulence in the whole plasma. In this paper, global behavior of the coupled system of the electromagnetic ITG turbulence and the zonal flows in tokamak plasmas is investigated

using a global electromagnetic Landau fluid code. The results of nonlinear simulations by the global code show that zonal flow behavior in tokamak plasmas depends on the safety factor q. In a low q ($q \sim 1$) region the zonal flows are stationary, and the zonal flows in the high q region are oscillatory. It is found that the difference of the zonal flow behavior leads to the different energy flow between the zonal flows and the turbulence. In the region where the stationary zonal flows are dominant, turbulence energy is transferred to the zonal flows via the Reynolds stress and the turbulence is suppressed by the zonal flows. On the other hand, the turbulence energy in the region with the oscillatory zonal flows is also transferred to the zonal flows via the Reynolds stress, but the zonal flow energy returns to the turbulence via the poloidally asymmetric pressure perturbations. Therefore the turbulent transport is not strongly suppressed in the oscillatory zonal flow region.

This paper is organized as follows. The model equation system is described in section 2. We consider the coupling of the GAMs and the zonal flows in section 3. In section 4, results of numerical calculations are given. Finally the obtained results are summarized in section 5.

2 Model Equations

We use 5-field (density n,electrostatic potential ϕ, parallel component of magnetic vector potential A, parallel ion velocity v and ion temperature T) Landau fluid equation system to describe the global electromagnetic turbulence in tokamak plasmas. Compared to the previous resistive drift-Alfvén model (3-field)[17], the equation system includes a parallel equation of motion for ion fluid and an ion temperature equation with Hammett-Perkins closure[18], and an electron Landau damping term is included in the Ohm's law[19]. In the electrostatic limit with adiabatic electrons the 5-field model reduces to the 3-field ion Landau fluid model in Refs. [20, 21, 22]. Nonlinear evolution equations for these fields are the following:

$$\begin{aligned}\frac{dn}{dt} &= a\frac{dn_{eq}}{dr}\nabla_\theta\phi - n_{eq}\nabla_\parallel v + \nabla_\parallel j \\ &\quad +\omega_d(n_{eq}\phi - p_e) + D_n\nabla_\perp^2 n \end{aligned} \tag{1}$$

$$\begin{aligned}\frac{d}{dt}\nabla_\perp^2\phi &= -T_{eq}\frac{a}{n_{eq}}\frac{dn_{eq}}{dr}(1+\eta_i)\nabla_\theta\nabla_\perp^2\phi + \frac{1}{n_{eq}}\nabla_\parallel j \\ &\quad -\omega_d\left(T_i + \frac{T_{eq}}{n_{eq}}n + \frac{p_e}{n_{eq}}\right) + D_U\nabla_\perp^4\phi \end{aligned} \tag{2}$$

$$\frac{dv}{dt} = -\nabla_\parallel T - (1+\tau)\frac{T_{eq}}{n_{eq}}\nabla_\parallel n - \beta T_{eq}\frac{a}{n_{eq}}\frac{dn_{eq}}{dr}(1+\eta_i+\tau)\nabla_\theta A + D_v\nabla_\perp^2 v \quad (3)$$

$$\beta\frac{\partial A}{\partial t} = -\nabla_\parallel\phi + \tau\frac{T_{eq}}{n_{eq}}\nabla_\parallel n + \beta\tau T_{eq}\frac{a}{n_{eq}}\frac{dn_{eq}}{dr}\nabla_\theta A + \sqrt{\frac{\pi}{2}\tau\frac{m_e}{m_i}}|\nabla_\parallel|\left(v - \frac{j}{n_{eq}}\right) - \eta j \quad (4)$$

$$\frac{dT}{dt} = T_{eq}\frac{a}{n_{eq}}\frac{dn_{eq}}{dr}\eta_i\nabla_\theta\phi - (\Gamma-1)T_{eq}\nabla_\parallel v + T_{eq}\omega_d\left((\Gamma-1)\phi + (2\Gamma-1)T + (\Gamma-1)\frac{T_{eq}}{n_{eq}}n\right) - (\Gamma-1)\sqrt{\frac{8T_{eq}}{\pi}}|\nabla_\parallel|T + D_T\nabla_\perp^2 T, \quad (5)$$

and parallel current is related with the magnetic potential through the Ampère's law

$$j = -\nabla_\perp^2 A, \quad (6)$$

where, $p_e = \tau T_{eq} n$, n_{eq} (T_{eq}) is an equilibrium density (ion temperature) normalized by the central value n_c (T_c), $\tau = T_{e0}/T_{i0}$ is a ratio of electron and ion equilibrium temperatures, $\beta = (n_c T_c)/(B_0^2/\mu_0)$ is a half of beta value evaluated on the plasma center, $\eta_i = d\ln T_{eq}/d\ln n_{eq}$, B_0 is a toroidal magnetic field on the magnetic axis and $\Gamma = 5/3$ is a ratio of specific heats. We assume a circular tokamak geometry (r,θ,ζ), where r is a radius of magnetic surface, θ and ζ are poloidal and toroidal angles, respectively. Then operators are defined as

$$\frac{df}{dt} = \partial_t f + [\phi, f], \quad \nabla_\parallel f = \epsilon\partial_\zeta f - \beta[A, f],$$

$$\omega_d \cdot f = 2\epsilon[r\cos\theta, f],$$

$$[f,g] = \frac{1}{r}\left(\frac{\partial f}{\partial r}\frac{\partial g}{\partial\theta} - \frac{\partial f}{\partial\theta}\frac{\partial g}{\partial r}\right)$$

where $\epsilon = a/R$ is an inverse aspect ratio, a and R are minor and major radii, respectively. Here the normalizations are $tv_{ti}/a \to t$, $r/\rho_i \to r$, $\rho_i\nabla_\perp \to \nabla_\perp$, $a\nabla_\parallel \to \nabla_\parallel$,

$$\frac{a}{\rho_i}\left(\frac{n}{n_c}, \frac{e\phi}{T_c}, \frac{v}{v_{ti}}, \frac{A}{\beta B_0\rho_i}, \frac{T}{T_c}\right) \to (n, \phi, v, A, T)$$

where $v_{ti} = \sqrt{T_c/m_i}$, $\rho_i = v_{ti}/\omega_{ci}$, $\omega_{ci} = eB_0/m_i$. Artificial disspations (D_n, D_U, D_v, D_T) are included to damp the small scale fluctuations.

3 Zonal Flow and Geodesic Acoustic Mode

In this section we analyze the coupling between the zonal flows and the GAMs in the present model briefly. The zonal flows can oscillate by the coupling with the (1,0) pressure perturbations. The zonal flow equation is obtained from flux surface average of the vorticity equation:

$$\frac{\partial \langle v_E \rangle}{\partial t} = -\frac{1}{r^2}\frac{\partial}{\partial r} r^2 \langle \tilde{v}_{Er} \tilde{v}_{E\theta} \rangle + \frac{\beta}{n_{eq}} \frac{1}{r^2} \frac{\partial}{\partial r} r^2 \langle \tilde{B}_r \tilde{B}_\theta \rangle - \frac{2}{n_{eq}} \frac{a}{R} \langle p \sin\theta \rangle, \tag{7}$$

where $\langle \cdot \rangle$ denotes the flux surface average, $\langle v_E \rangle = \frac{\partial \phi_0}{\partial r}$ is the zonal flow, $\tilde{v}_{Er} = -\frac{1}{r}\frac{\partial \tilde{\phi}}{\partial \theta}$ and $\tilde{v}_{E\theta} = \frac{\partial \tilde{\phi}}{\partial r}$ are E×B drift velocities in radial and poloidal directions, respectively, $\langle p \sin\theta \rangle$ is the (1,0) pressure perturbation and $p = p_i + p_e = n_{eq}T + T_{eq}n + \tau T_{eq} n$. In Eq. (7) a viscous term is neglected. The first and second terms in the right hand side are Reynolds and Maxwell stress terms, respectively. The zonal flows are directly connected with the turbulence through these stress terms. The final term shows the coupling with the (1,0) pressure perturbations due to the geodesic curvature.

The equation for the (1,0) total pressure perturbation is expressed as

$$\frac{\partial}{\partial t} \langle p \sin\theta \rangle = -\langle [\tilde{\phi}, \tilde{p}] \sin\theta \rangle + (\Gamma + \tau) p_{eq} \frac{a}{qR} \langle v \cos\theta \rangle + (\Gamma + \tau) \frac{a}{R} p_{eq} \langle v_E \rangle. \tag{8}$$

Here magnetic nonlinearity ($[\tilde{A}, \tilde{v}]$, $[\tilde{A}, \tilde{j}]$) related terms, Alfvén waves ($\langle j \cos\theta \rangle$ term), coupling with the (2,0) mode ($\langle \phi \cos 2\theta \rangle$, $\langle v_E \cos 2\theta \rangle$ terms) and Landau damping term are neglected. The first term in the right hand side shows a nonlinear coupling with the turbulence. Recently it has been reported that zonal flows are driven by $\langle p \sin\theta \rangle$ generated from the turbulence through the nonlinear term, which was the result from the three-dimensional electrostatic Braginskii turbulence simulations in the core/edge transition regime[11]. On the other hand, the 4-field drift-Alfvén turbulence simulations in the edge region have shown that zonal flow energy is transferred back to the turbulence through this term [13]. We also investigate this point in our nonlinear simulations. From the terms including $\langle v_E \rangle$ and $\langle p \sin\theta \rangle$ in Eqs. (7) and (8), we obtain the GAM oscillation equation,

$$\frac{\partial^2 \langle v_E \rangle}{\partial t^2} = -2(\Gamma + \tau) T_{eq} \left(\frac{a}{R}\right)^2 \langle v_E \rangle. \tag{9}$$

Replacing $\partial_t \to -i\hat{\omega}$ yields the normalized GAM frequency,

$$\hat{\omega}_{\rm GAM} = \sqrt{2(\Gamma+\tau)T_{eq}}\frac{a}{R}. \tag{10}$$

Since time is normalizd by a/v_{ti}, the GAM frequency in physical unit is $\sim v_{ti}/R$. In the same way, from the terms including $\langle p\sin\theta\rangle$ and $\langle v\cos\theta\rangle$ in Eq. (8) and the equation for $\langle v\cos\theta\rangle$ described by

$$\frac{\partial}{\partial t}\langle v\cos\theta\rangle = -\frac{1}{n_{eq}}\frac{a}{qR}\langle p\sin\theta\rangle, \tag{11}$$

we obtain the normalized parallel sound wave frequency for the (1,0) mode,

$$\hat{\omega}_{\rm sound} = \sqrt{(\Gamma+\tau)T_{eq}}\frac{a}{qR}. \tag{12}$$

For the (1,0) mode, the timescale of the dynamics parallel to the magnetic field is represented by $\hat{\omega}^{-1}_{\rm sound}$. The zonal flows are usually driven by the turbulence via the Reynolds stress and tend to excite the (1,0) pressure perturbations $\langle p\sin\theta\rangle$ in toroidal system. In a high q region where the sound waves are negligible, the zonal flows can excite the (1,0) pressure perturbations which change the direction of the zonal flows, and then the zonal flows oscillate with the (1,0) pressure perturbations at $\hat{\omega}_{\rm GAM}$. On the other hand, when $\hat{\omega}_{\rm sound}$ is close to $\hat{\omega}_{\rm GAM}$ at low q ($q\sim 1$), the sound wave term in Eq. (8) becomes comparable to the term including $\langle v_E\rangle$. In this case, the (1,0) pressure perturbations are relaxed along the magnetic field by the sound waves due to short connection length qR as soon as the zonal flows excite the (1,0) pressure perturbations. The zonal flows cannot oscillate without the (1,0) pressure perturbations, so that the zonal flows are stationary in a low q region. Thus the safety factor q is important for the zonal flow behavior in toroidal system.

4 Numerical Results

Parameters used in the calculations are $R/a = 4$, $\rho_i/a = 0.0125$, $\tau = 1$, $\beta = 0.001$, $n_{eq} = 0.8 + 0.2e^{-2(r/a)^2}$, $T_{eq} = 0.35 + 0.65(1-(r/a)^2)^2$, $q = 1.05 + 2(r/a)^2$. These background profiles shown in Fig. 1 are fixed in the calculations. All fluctuations are expanded in Fourier modes in the poloidal and toroidal directions,

$$f = \sum_{m,n} f_{mn}(r,t)\exp[i(m\theta - n\zeta)] \tag{13}$$

and finite differenciated in the radial direction. The Fourier modes included in the calculations are ones having resonant surfaces between $0.2 < r/a < 0.8$ in the range of

$m \leqq 80$ and $n \leqq 50$, and nonresonant $(m,n) = (0,0),(1,0)$ components. Only even toroidal modes are kept to save computational time. The number of radial mesh is 256. Artificial disspations (D_n, D_U, D_v, D_T) depend on the poloidal mode number m and are set to be $\sim 10^{-7}m^4$, and resistivity $\eta = 4 \times 10^{-5}$. The dominant instability in the present parameters is the ITG mode.

4.1 Two Types of Zonal Flows

Figure 2 shows the temporal evolution of the zonal flows in quasi steady state. Zonal flow behavior changes with radius. In the inner (low q) region ($r/a < 0.5$) the zonal flows are almost stationary. On the other hand, the zonal flows make a coherent oscillation due to the coupling with the GAM in the outer (high q) region. The difference of the zonal flow frequency is clearly seen in Fig. 3, in which the pure GAM frequency $f_{\rm GAM} = \hat{\omega}_{\rm GAM}/2\pi$ and the pure parallel sound frequency $f_{\rm sound} = \hat{\omega}_{\rm sound}/2\pi$ are also plotted. In the inner region there are two large peaks around zero frequency, which correspond to the stationary sheared zonal flow. On the other hand, the zonal flows in the outer region have finite frequency. Although there are small peaks along $f_{\rm GAM}$, main peaks are located at $f = 0.04 - 0.05$, which is lower than $f_{\rm GAM}$. When $f_{\rm sound}$ is the same as the frequency of the oscillatory zonal flows by decreasing q, the zonal flows change from the oscillatory mode to the stationary mode.

4.2 Energy Loop Between Zonal Flows and Turbulence

In this subsection energy flow between the zonal flows and the turbulence is investigated in detail. Multiplying $\langle v_E \rangle$ to Eq. (7), we obtain the zonal flow energy equation,

$$\frac{\partial}{\partial t}\frac{1}{2}\langle v_E \rangle^2 = \underbrace{-\langle \tilde{v}_{Er}\tilde{\Omega}\rangle\langle v_E\rangle}_{\text{Reynolds}} + \underbrace{\hat{\beta}\langle \tilde{B}_r\tilde{j}\rangle\langle v_E\rangle}_{\text{Maxwell}} \underbrace{-\omega_B\langle p\sin\theta\rangle\langle v_E\rangle}_{\text{geodesic transfer}}, \tag{14}$$

where $\tilde{\Omega} = \nabla_\perp^2\tilde{\phi}$ is vorticity and $\omega_B = 2a/R$. Figure 4 shows temporal evolution of three terms in the right hand side of the above equation at (a) $r/a = 0.31$ and (b) $r/a = 0.65$ and the time averaged values are listed in Table 1. At $r/a = 0.31$ where the zonal flows are stationary, the Reynolds stress term is almost always positive and transfer energy from the turbulence to the zonal flows. While the geodesic transfer term is negative and energy of the zonal flows goes to the (m,n)=(1,0) pressure perturbations $\langle p\sin\theta\rangle$. At $r/a = 0.65$ where the zonal flows are oscillatory, the mean Reynolds stress contribution is positive. The zonal flow energy is supplied averagely through the Reynolds stress drive

from the turbulence. It is noted that the mean Reynolds stress drive at $r/a = 0.31$ is larger than that at $r/a = 0.65$, although turbulence level at $r/a = 0.65$ is higher than that at $r/a = 0.31$. The oscillatory nature of the zonal flows makes the mean drive less effective. The geodesic transfer term is dominant at $r/a = 0.65$ and takes both positive and negative values temporally as shown in Fig. 4 (b). The mean geodesic transfer effect is negative, so that the zonal flow energy goes to the (1,0) pressure perturbations averagely.

The Maxwell stress contribution is very small compared to the other contributions, but it increases with β[23]. Therefore, the Maxwell stress may affect the zonal flow generation in high β plasmas.

The zonal flow energy is transferred mainly to the (1,0) ion pressure perturbations. The equation describing time evolution of the (1,0) ion pressure perturbation energy is

$$\begin{aligned}\frac{\partial}{\partial t}\frac{1}{2}\langle p_i \sin\theta\rangle^2 = & \underbrace{-\langle[\tilde{\phi},\tilde{p}_i]\sin\theta\rangle\langle p_i\sin\theta\rangle}_{\text{nonlinear transfer}} \\ & \underbrace{+\Gamma p_{eq}\frac{a}{qR}\langle v\cos\theta\rangle\langle p_i\sin\theta\rangle}_{\text{sound wave}} \\ & \underbrace{-(\Gamma-1)\sqrt{\frac{8T_{eq}}{\pi}}|k_\parallel|\langle T\sin\theta\rangle\langle p_i\sin\theta\rangle}_{\text{Landau damping}} \\ & \underbrace{+\Gamma p_{eq}\frac{a}{R}\langle v_E\rangle\langle p_i\sin\theta\rangle}_{\text{zonal flow}}. \end{aligned} \tag{15}$$

Here magnetic nonlinearity and source from the equilibrium pressure gradient are neglected. Figure 5 shows the temporal evolution of nonlinear transfer, sound wave and zonal flow terms in the right hand side of the above equation at (a) $r/a = 0.31$ and (b) $r/a = 0.65$. The time averaged values are also listed in Table 2. At $r/a = 0.31$ the zonal flow term is almost always balanced by the sound wave term, and the energy transferred from the zonal flows goes to the parallel sound waves. The nonlinear energy transfer is very small at $r/a = 0.31$, so that the energy hardly returns to the turbulence. On the other hand, the nonlinear energy transfer to the turbulence is significant at $r/a = 0.65$. The energy loop between the zonal flows and the turbulence via the (1,0) pressure perturbations is formed in the high q region as pointed out in Ref. [13]. Therefore it is difficult that the zonal flows increase over the turbulence. As a result, a difference of the ratio $E_{k,ZF}/(E_{k,ZF}+E_{k,turb})$ appears in the plasma as shown in Fig. 6, where $E_{k,ZF} = \frac{1}{2}\langle v_E\rangle^2$ is the zonal flow energy and $E_{k,turb} = \frac{1}{2}|\nabla_\perp\tilde{\phi}|^2$ is the kinetic energy of the turbulence. In the low q region ($r/a < 0.45$) where the zonal flows are stationary, the zonal flows are

dominant to the turbulence. While, in the high q region ($r/a > 0.45$) where the zonal flows are oscillatory, the zonal flow level is same as the turbulence due to the energy loop between the zonal flows and the turbulence.

Figure 7 shows temporal evolution of electrostatic component of heat flux $\langle \tilde{T}\tilde{v}_{Er} \rangle$, The heat transport is effectively suppressed in the inner zonal flow dominant region. On the other hand, the heat flux in the outer region is not small, because the zonal flow level is same as the turbulence level. Besides, the effective shearing rate of the oscillatory zonal flows is smaller than that of the stationary zonal flows[16]. This leads to weak suppression of the heat flux by the oscillatory zonal flows.

5 Summary

Using the developed global Landau-fluid code, we have performed the electromagnetic ITG turbulence simulations in tokamak plasmas. Two types of zonal flows, stationary and oscillatory modes, are possible in toroidal system. The zonal flow behavior is changed by the safety factor q. In the low q region the zonal flows are stationary. The stationary zonal flows suppress the turbulence efficiently. On the other hand, the zonal flows are oscillatory in the high q region due to the coupling with the (1,0) pressure perturbations. The oscillatory nature makes the suppression of the turbulence by the zonal flows less effective. The zonal flows are driven from the turbulence via the Reynolds stress. A part of the energy of the oscillatory zonal flows is transferred back to the turbulence through the (1,0) pressure perturbations. Therefore the oscillatory zonal flows cannot quench the turbulence unlike the stationary zonal flows whose energy hardly returns to the turbulence.

Thus the stationary zonal flows are favorable for the turbulence suppression from the point of view of both their timescale and energy flow. These results may be helpful in understanding experimentally observed internal transport barriers (ITBs) in tokamak plasmas with positive magnetic shear, although to demonstrate the relation with the ITB formation the analysis with neoclassical effect and heating is necessary like in Refs [22, 25, 24].

Acknowledgements

The authors (especially N. M.) would like to thank M. Yagi, H. Sugama, P. B. Snyder, J. Candy and G. R. McKee for helpful suggestions and discussions on this work. We also thank M. Kikuchi and H. Ninomiya for fruitful discussions.

References

[1] A. Hasegawa and M. Wakatani, Phys. Rev. Lett. **59**, 1581 (1987).

[2] Z. Lin, T. S. Hahm, W. W. Lee, W. M. Tang and P. H. Diamond, Phys. Rev. Lett. **83**, 3645 (1999).

[3] P. H. Diamond, M. N. Rosenbluth, F. L. Hinton, M. Malkov, J. Fleischer and A. Smolyakov, in *Plasma Physics and Controlled Nuclear Fusion Research*, 17th IAEA Fusion Energy Conference, Yokohama, Japan, 1998 (IAEA, Vienna, 1998), p. IAEA-CN-69/TH3/1.

[4] P. H. Diamond, S. Champeaux, M. Malkov, A. Das, I. Gruzinov, M. N. Rosenbluth, C. Holland, B. Wecht, A. I. Smolyakov, F. L. Hinton, Z. Lin and T. S. Hahm, Nucl. Fusion **41**, 1067 (2001).

[5] A. I. Smolyakov, P. H. Diamond and M. V. Medvedev, Phys. Plasmas **7**, 3987 (2000).

[6] P. N. Guzdar, R. G. Kleva, A. Das and P. K. Kaw, Phys. Rev. Lett. **87**, 15001 (2001).

[7] L. Chen, Z. Lin, R. B. White and F. Zonca, Nucl. Fusion **41**, 747 (2001).

[8] J. Anderson, H. Nordman, R. Singh and J. Weiland, Phys. Plasmas **9**, 4500 (2002).

[9] V. P. Lakhin, Plasma Phys. Rep. **29**, 137 (2003).

[10] N. Winsor, J. L. Johnson and J. M. Dawson, Phys. Fluids **11**, 2448 (1968).

[11] K. Hallatschek and D. Biskamp, Phys. Rev. Lett. **86**, 1223 (2001).

[12] M. Ramisch, U. Stroth, S. Niedner and B. Scott, New J. Phys. **5**, 12.1 (2003).

[13] B. Scott, Phys. Lett. A **320**, 53 (2003).

[14] P. M. Schoch, "Experimental evidence of zonal flows using HIBP data", submitted to Phys. Rev. Lett.

[15] G. R. McKee, R. J. Fonck, M. Jakubowski, K. H. Burrell, K. Hallatschek, R. A. Moyer, D. L. Rudakov, W. Nevins, G. D. Porter, P. Schoch and X. Xu, Phys. Plasmas **10** 1712 (2003).

[16] T. S. Hahm, M. A. Beer, Z. Lin, G. W. Hammett, W. W. Lee and W. M. Tang, Phys. Plasmas **6**, 922 (1999).

[17] N. Miyato, S. Hamaguchi and M. Wakatani, Plasma Phys. Controlled Fusion **44**, 1689 (2002).

[18] G. W. Hammett and F. W. Perkins, Phys. Rev. Lett. **64**, 3019 (1990).

[19] P. B. Snyder and G. W. Hammett, Phys. Plasmas **8**, 3199 (2001).

[20] N. Mattor, Phys. Fluid B **4**, 3952 (1992).

[21] J. N. Leboeuf, V. E. Lynch, B. A. Carreras, J. D. Alvarez and L. Garcia, Phys. Plasmas **7**, 5013 (2000).

[22] X. Garbet, C. Bourdelle, G. T. Hoang, P. Maget, S. Benkadda, P. Beyer, C. Figarella, I. Voitsekovitch, O. Agullo and N. Bian, Phys. Plasmas **8**, 2793 (2001).

[23] N. Miyato, J. Li and Y. Kishimoto, to be published in J. Plasma Fusion Res. SERIES **6** (2004).

[24] I. Voitsekhovitch, X. Garbet, S. Benkadda, P. Beyer and C. F. Figarella, Phys. Plasmas **9**, 4671 (2002).

[25] A. Thyagaraja, Plasma Phys. Controlled Fusion **42**, B255 (2000).

Table 1: Time averaged zonal flow energy drives due to Reynolds stress, Maxwell stress and geodesic transfer effect in Eq. (14).

	r/a=0.31	r/a=0.65
Reynolds drive	1.47×10^{-2}	1.01×10^{-2}
Maxwell drive	5.01×10^{-4}	-2.75×10^{-3}
Geodesic transfer	-1.24×10^{-2}	-7.56×10^{-3}

Table 2: Time averaged contributions to the (1,0) ion pressure perturbation energy in Eq. (15).

	r/a=0.31	r/a=0.65
Nonlinear	-8.83×10^{-5}	-1.51×10^{-3}
Sound wave	-2.20×10^{-3}	-6.45×10^{-4}
Zonal flow	2.51×10^{-3}	3.38×10^{-3}
Landau damping	-1.19×10^{-4}	-1.91×10^{-3}

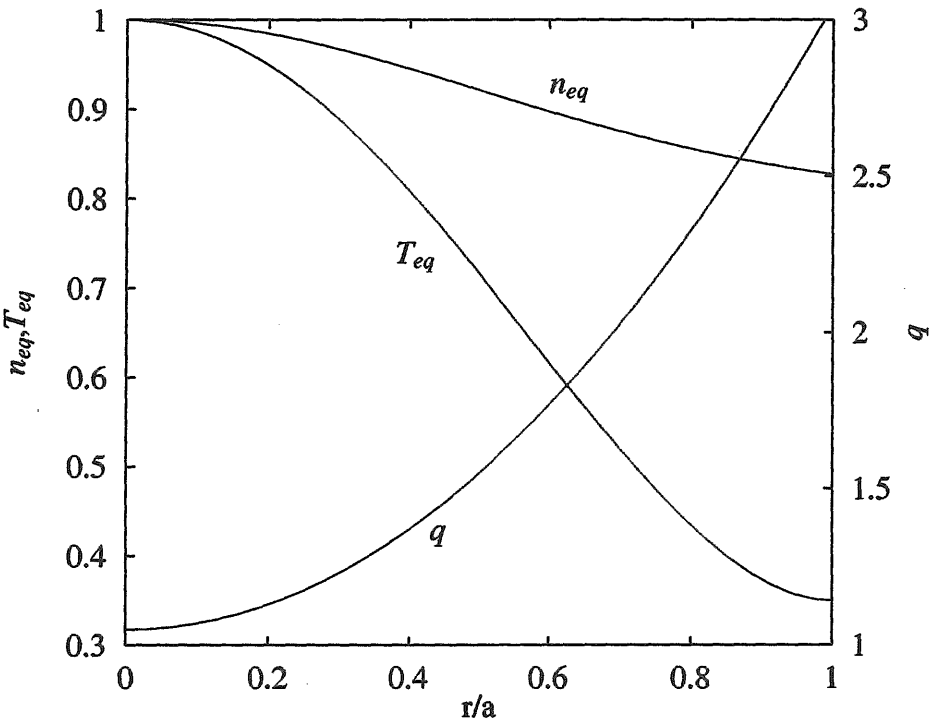

Figure 1: Normalized density, temperature and safety factor profiles.

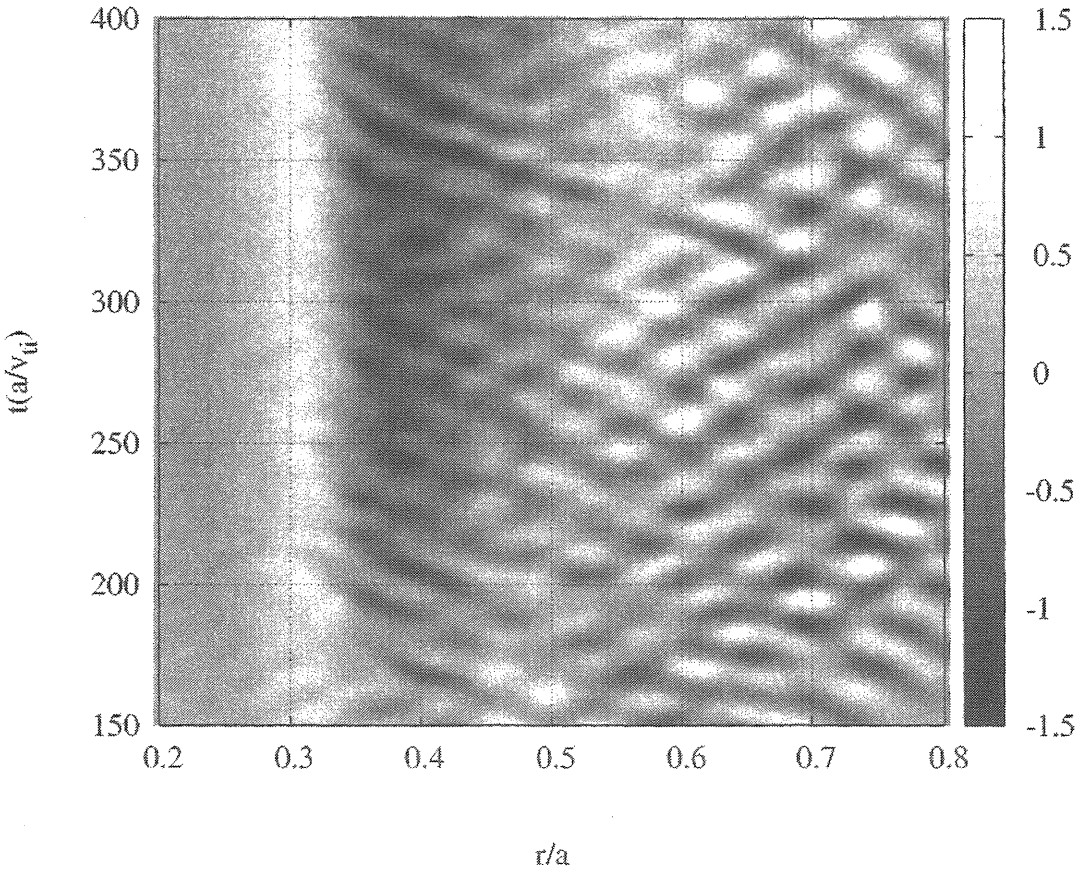

Figure 2: Temporal evolution of zonal flows $\langle v_E \rangle$.

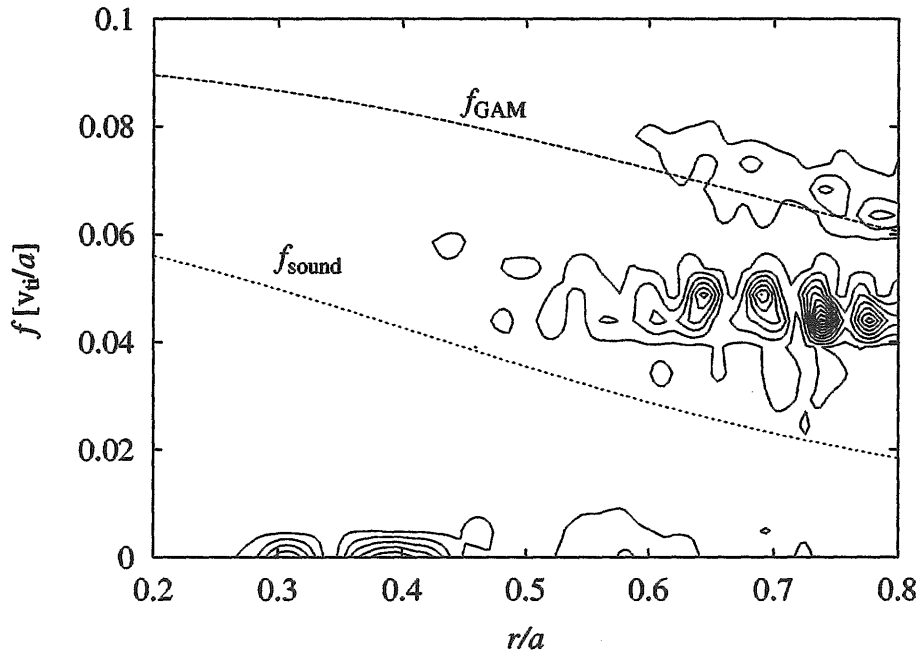

Figure 3: Radial variation of zonal flow frequency. Frequency is normalized by a/v_{ti}. The pure GAM frequency $f_{\rm GAM} = \hat{\omega}_{\rm GAM}/2\pi$ and the pure sound wave frequency $f_{\rm sound} = \hat{\omega}_{\rm sound}/2\pi$ are also plotted.

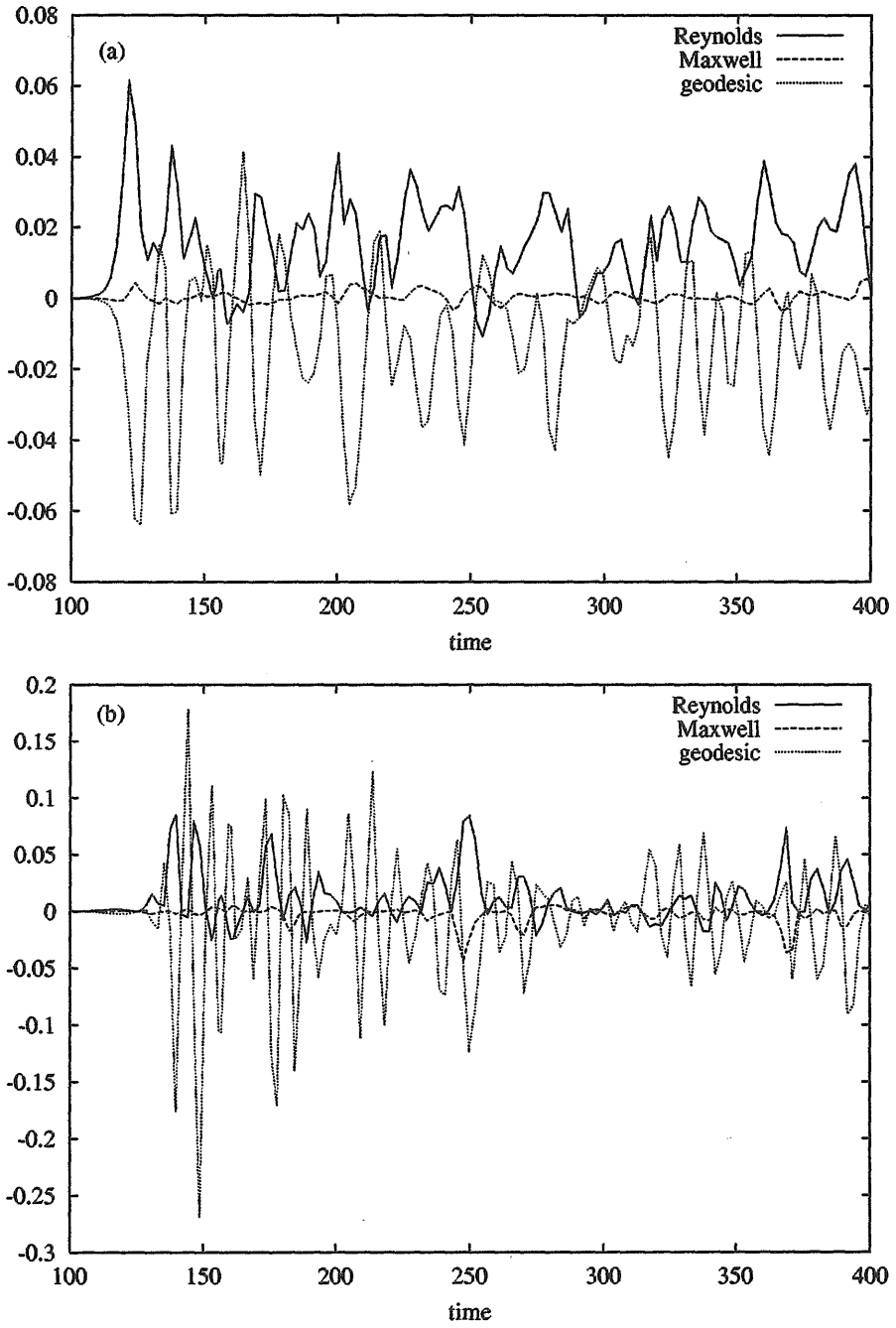

Figure 4: Temporal evolution of zonal flow energy drives in Eq. (14) at (a) r/a=0.31 and (b) r/a=0.65.

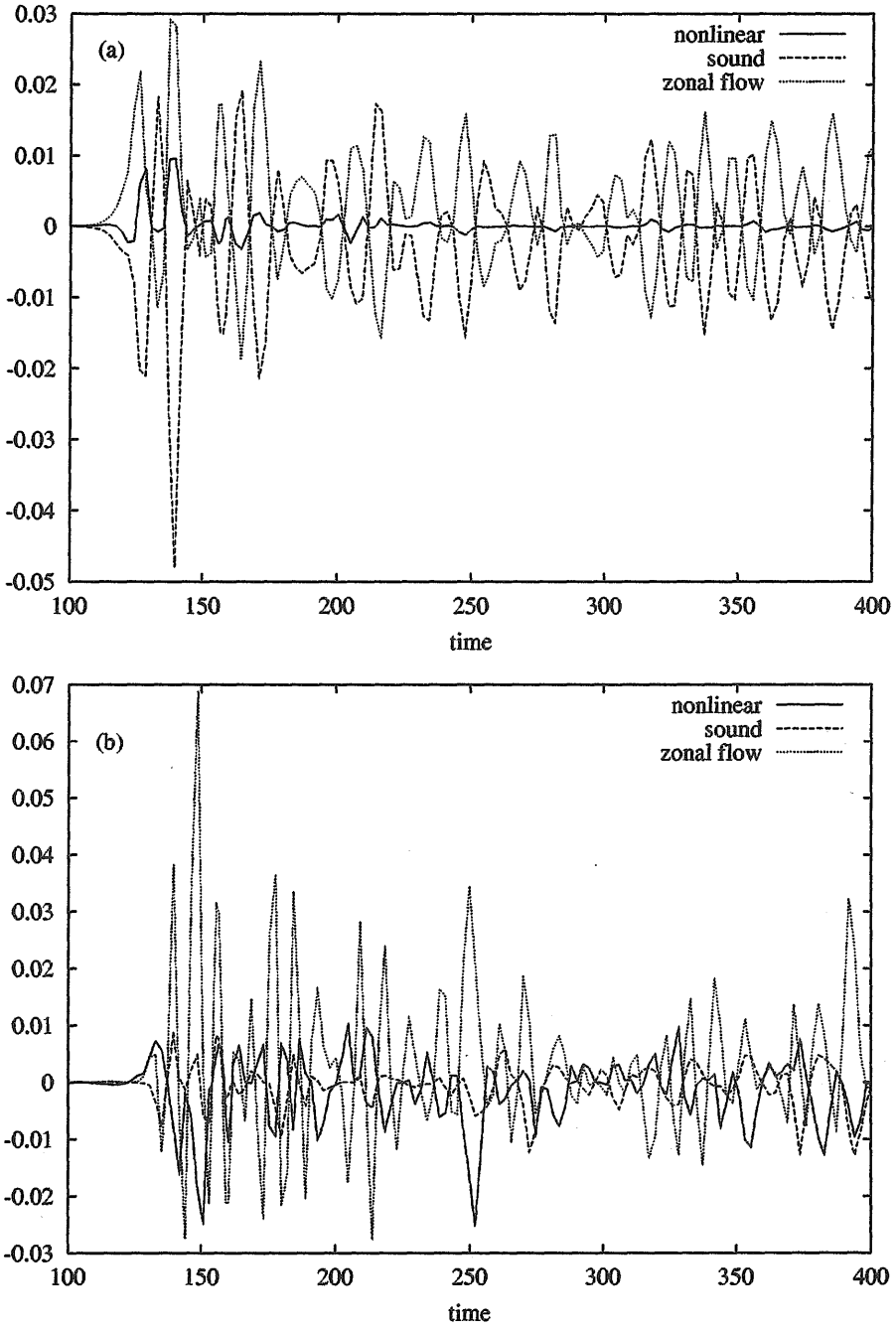

Figure 5: Temporal evolution of $\langle p_i \sin\theta \rangle$ energy drives in Eq. (15) at (a) r/a=0.31 and (b) r/a=0.65.

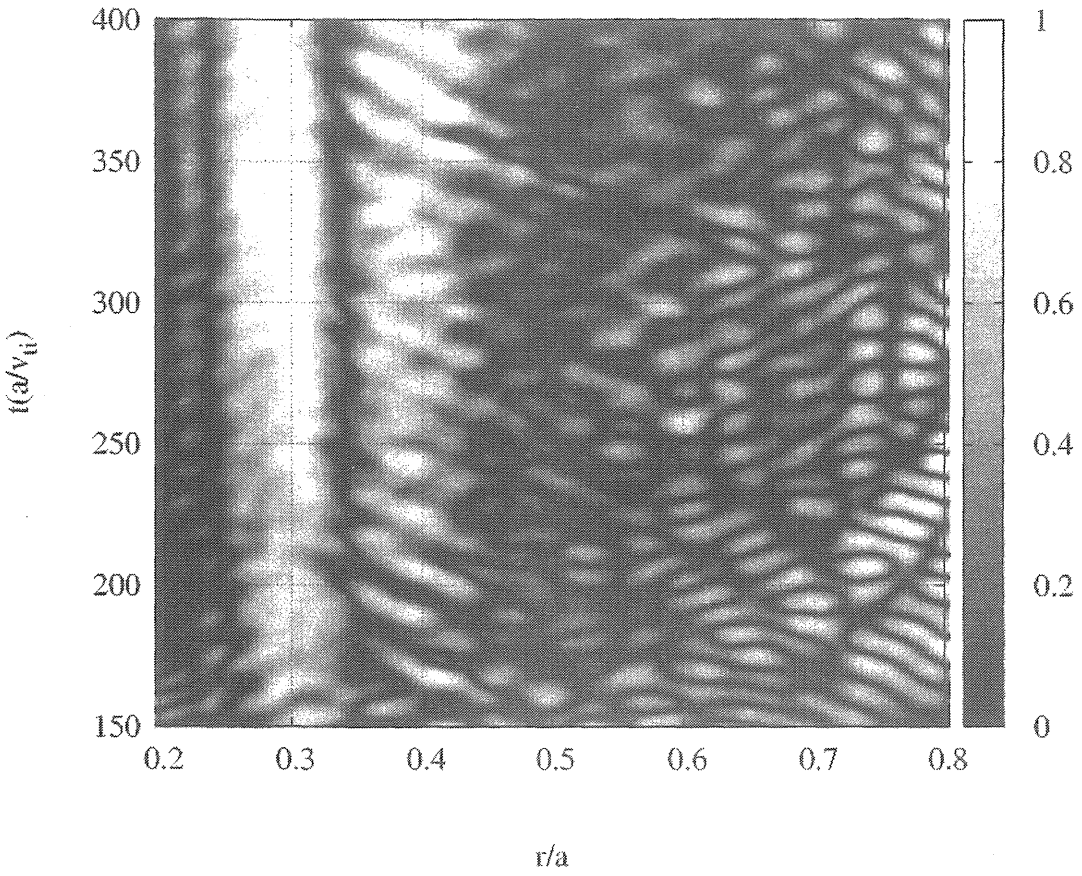

Figure 6: Temporal evolution of the ratio $E_{k,ZF}/(E_{k,ZF} + E_{k,turb})$.

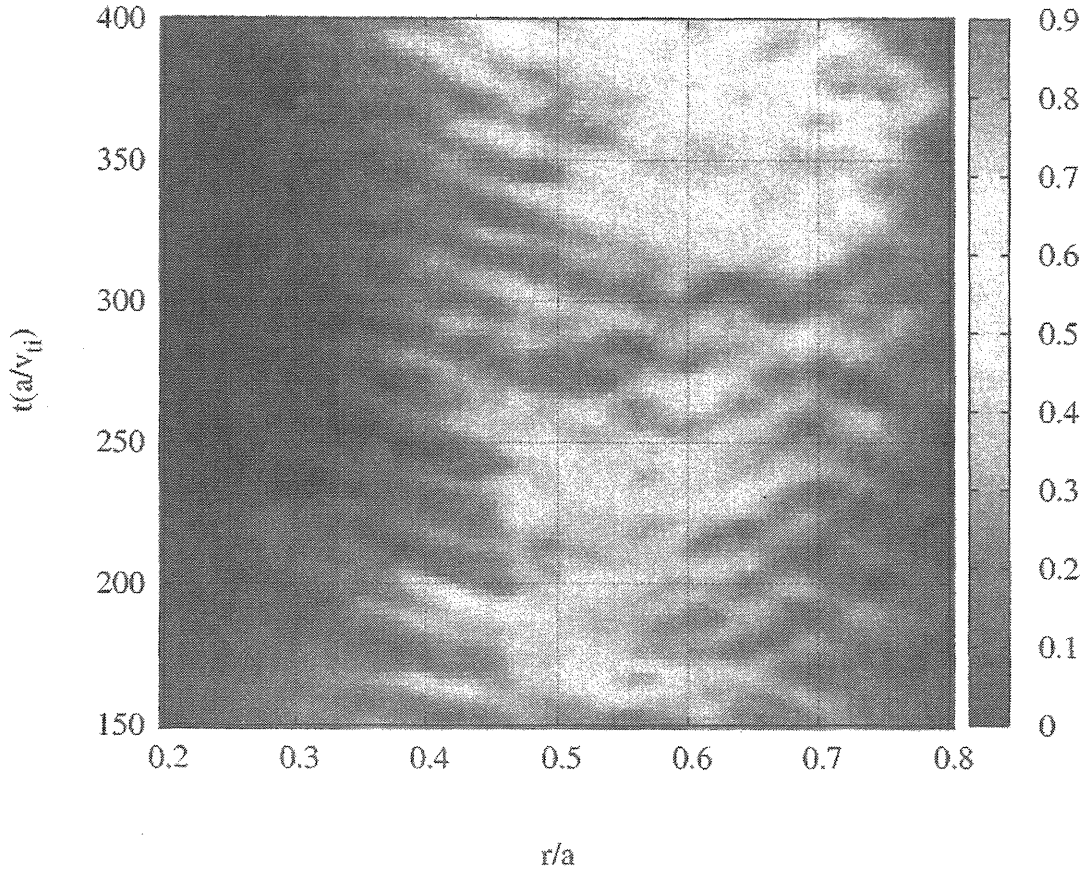

Figure 7: Temporal evolution of electrostatic component of heat flux.

国際単位系 (SI) と換算表

表 1　SI基本単位および補助単位

量	名称	記号
長さ	メートル	m
質量	キログラム	kg
時間	秒	s
電流	アンペア	A
熱力学温度	ケルビン	K
物質量	モル	mol
光度	カンデラ	cd
平面角	ラジアン	rad
立体角	ステラジアン	sr

表 2　SIと併用される単位

名称	記号
分，時，日	min, h, d
度，分，秒	°, ′, ″
リットル	l, L
トン	t
電子ボルト	eV
原子質量単位	u

1 eV = 1.60218 × 10^{-19} J

1 u = 1.66054 × 10^{-27} kg

表 5　SI接頭語

倍数	接頭語	記号
10^{18}	エクサ	E
10^{15}	ペタ	P
10^{12}	テラ	T
10^{9}	ギガ	G
10^{6}	メガ	M
10^{3}	キロ	k
10^{2}	ヘクト	h
10^{1}	デカ	da
10^{-1}	デシ	d
10^{-2}	センチ	c
10^{-3}	ミリ	m
10^{-6}	マイクロ	μ
10^{-9}	ナノ	n
10^{-12}	ピコ	p
10^{-15}	フェムト	f
10^{-18}	アト	a

表 3　固有の名称をもつSI組立単位

量	名称	記号	他のSI単位による表現
周波数	ヘルツ	Hz	s^{-1}
力	ニュートン	N	m·kg/s^2
圧力，応力	パスカル	Pa	N/m^2
エネルギー，仕事，熱量	ジュール	J	N·m
工率，放射束	ワット	W	J/s
電気量，電荷	クーロン	C	A·s
電位，電圧，起電力	ボルト	V	W/A
静電容量	ファラド	F	C/V
電気抵抗	オーム	Ω	V/A
コンダクタンス	ジーメンス	S	A/V
磁束	ウェーバ	Wb	V·s
磁束密度	テスラ	T	Wb/m^2
インダクタンス	ヘンリー	H	Wb/A
セルシウス温度	セルシウス度	℃	
光束	ルーメン	lm	cd·sr
照度	ルクス	lx	lm/m^2
放射能	ベクレル	Bq	s^{-1}
吸収線量	グレイ	Gy	J/kg
線量当量	シーベルト	Sv	J/kg

表 4　SIと共に暫定的に維持される単位

名称	記号
オングストローム	Å
バーン	b
バール	bar
ガル	Gal
キュリー	Ci
レントゲン	R
ラド	rad
レム	rem

1 Å = 0.1 nm = 10^{-10} m

1 b = 100 fm^2 = 10^{-28} m^2

1 bar = 0.1 MPa = 10^5 Pa

1 Gal = 1 cm/s^2 = 10^{-2} m/s^2

1 Ci = 3.7 × 10^{10} Bq

1 R = 2.58 × 10^{-4} C/kg

1 rad = 1 cGy = 10^{-2} Gy

1 rem = 1 cSv = 10^{-2} Sv

（注）

1. 表1－5は「国際単位系」第5版，国際度量衡局 1985年刊行による。ただし，1 eVおよび1 uの値はCODATAの1986年推奨値によった。
2. 表4には海里，ノット，アール，ヘクタールも含まれているが日常の単位なのでここでは省略した。
3. barは，JISでは流体の圧力を表わす場合に限り表2のカテゴリーに分類されている。
4. EC閣僚理事会指令ではbar，barnおよび「血圧の単位」mmHgを表2のカテゴリーに入れている。

換　算　表

力	N(=10^5 dyn)	kgf	lbf
	1	0.101972	0.224809
	9.80665	1	2.20462
	4.44822	0.453592	1

粘度　1 Pa·s(N·s/m^2) = 10 P(ポアズ)(g/(cm·s))

動粘度　1 m^2/s = 10^4 St(ストークス)(cm^2/s)

圧力	MPa(=10 bar)	kgf/cm^2	atm	mmHg(Torr)	lbf/in^2(psi)
	1	10.1972	9.86923	7.50062 × 10^3	145.038
	0.0980665	1	0.967841	735.559	14.2233
	0.101325	1.03323	1	760	14.6959
	1.33322 × 10^{-4}	1.35951 × 10^{-3}	1.31579 × 10^{-3}	1	1.93368 × 10^{-2}
	6.89476 × 10^{-3}	7.03070 × 10^{-2}	6.80460 × 10^{-2}	51.7149	1

エネルギー・仕事・熱量	J(=10^7 erg)	kgf·m	kW·h	cal(計量法)	Btu	ft·lbf	eV
	1	0.101972	2.77778 × 10^{-7}	0.238889	9.47813 × 10^{-4}	0.737562	6.24150 × 10^{18}
	9.80665	1	2.72407 × 10^{-6}	2.34270	9.29487 × 10^{-3}	7.23301	6.12082 × 10^{19}
	3.6 × 10^6	3.67098 × 10^5	1	8.59999 × 10^5	3412.13	2.65522 × 10^6	2.24694 × 10^{25}
	4.18605	0.426858	1.16279 × 10^{-6}	1	3.96759 × 10^{-3}	3.08747	2.61272 × 10^{19}
	1055.06	107.586	2.93072 × 10^{-4}	252.042	1	778.172	6.58515 × 10^{21}
	1.35582	0.138255	3.76616 × 10^{-7}	0.323890	1.28506 × 10^{-3}	1	8.46233 × 10^{18}
	1.60218 × 10^{-19}	1.63377 × 10^{-20}	4.45050 × 10^{-26}	3.82743 × 10^{-20}	1.51857 × 10^{-22}	1.18171 × 10^{-19}	1

1 cal = 4.18605 J (計量法)
= 4.184 J (熱化学)
= 4.1855 J (15 °C)
= 4.1868 J (国際蒸気表)

仕事率　1 PS (仏馬力)
= 75 kgf·m/s
= 735.499 W

放射能	Bq	Ci
	1	2.70270 × 10^{-11}
	3.7 × 10^{10}	1

吸収線量	Gy	rad
	1	100
	0.01	1

照射線量	C/kg	R
	1	3876
	2.58 × 10^{-4}	1

線量当量	Sv	rem
	1	100
	0.01	1

(86年12月26日現在)

Global Characteristics of Zonal Flows Generated by Ion Temperature Gradient Driven Turbulence in Tokamak Plasmas